Published online 9 September 2011

Nucleic Acids Research, 2012, Vol. 40, No. 1 ***65–74***
doi:10.1093/nar/gkr649

Genome-wide H4 K16 acetylation by SAS-I is deposited independently of transcription and histone exchange

Franziska Heise[1], Ho-Ryun Chung[2], Jan M. Weber[1], Zhenyu Xu[3], Ludger Klein-Hitpass[4], Lars M. Steinmetz[3], Martin Vingron[2] and Ann E. Ehrenhofer-Murray[1,*]

[1]Zentrum für Medizinische Biotechnologie, Abteilung Genetik, Universität Duisburg-Essen, Essen, [2]Max-Planck-Institut für molekulare Genetik, Department of Computational Molecular Biology, Ihnestraße 73, 14195 Berlin, [3]European Molecular Biology Laboratory, Meyerhofstraße 1, 69117 Heidelberg and [4]Institut für Zellbiologie, Universitätsklinikum Essen, Virchowstraße 173, 45122 Essen, Germany

Received February 21, 2011; Revised July 13, 2011; Accepted July 24, 2011

ABSTRACT

The MYST HAT Sas2 is part of the SAS-I complex that acetylates histone H4 lysine 16 (H4 K16Ac) and blocks the propagation of heterochromatin at the telomeres of *Saccharomyces cerevisiae*. In this study, we investigated Sas2-mediated H4 K16Ac on a genome-wide scale. Interestingly, H4 K16Ac loss in *sas2Δ* cells outside of the telomeric regions showed a distinctive pattern in that there was a pronounced decrease of H4 K16Ac within the majority of open reading frames (ORFs), but little change in intergenic regions. Furthermore, regions of low histone H3 exchange and low H3 K56 acetylation showed the most pronounced loss of H4 K16Ac in *sas2Δ*, indicating that Sas2 deposited this modification on chromatin independently of histone exchange. In agreement with the effect of Sas2 within ORFs, *sas2Δ* caused resistance to 6-azauracil, indicating a positive effect on transcription elongation in the absence of H4 K16Ac. In summary, our data suggest that Sas2-dependent H4 K16Ac is deposited into chromatin independently of transcription and histone exchange, and that it has an inhibitory effect on the ability of PolII to travel through the body of the gene.

INTRODUCTION

Chromatin function is modulated by a wide variety of post-translational modifications (PTMs) on the histones, among which acetylation has been extensively studied (1). Selected histone acetyltransferases (HATs) are recruited via DNA binding proteins to gene promoters, where they cooperate with other chromatin regulators in transcriptional activation (2). As the RNA polymerase II (PolII) proceeds along the body of the gene during transcription elongation, it uses several accessory factors as well as histone modifying activities to navigate through the chromatin (3). Furthermore, transcription through a gene is accompanied by the eviction and redeposition of H2A/ H2B and H3/ H4 by the histone chaperones FACT (4) and Asf1 (5), respectively. Interestingly, there also is widespread replication- and transcription-independent exchange of H3 at gene promoters by Asf1 (5–7), and such deposited histones are acetylated on H3 K56 (6).

While some types of histone modifications are directed to a particular genomic location by the interaction of a chromatin-modifying complex with a DNA binding factor or PolII, other modifications are more globally deposited in the genome. One histone modifying complex that may follow this latter pattern is the HAT complex SAS-I, which consists of the subunits Sas2, Sas4 and Sas5 (8,9) and acetylates H4 K16 (10). The absence of SAS-I causes a marked, but not complete, reduction of H4 K16 acetylation on bulk histones (11), and at least some of the remaining H4 K16Ac is carried out by NuA4/ Esa1 (12). Since the H4 K16 acetylation mark deposited by SAS-I is particularly important to counteract the activity of the Sir2 HDAC and the binding of the heterochromatic SIR complex to chromatin (13), its absence in *sas2Δ* cells causes a redistribution of the SIR complexes to more centromere-proximal regions (11,12), which is lethal in combination with another boundary factor, the HDAC complex Rpd3(L) (14). SAS-I-mediated acetylation is also required for the incorporation of H2A.Z in subtelomeric chromatin, which contributes to its anti-silencing function (15). In agreement with these findings, deletions of SAS-I components cause a loss of telomeric silencing (16) and increased repression of genes located in subtelomeric regions (11,12). Interestingly, this also has an impact on the replicative lifespan of yeast (17).

*To whom correspondence should be addressed. Tel: + 49 201 183 4132; Fax: + 49 201 183 4397; Email: ann.ehrenhofer-murray@uni-due.de

In addition to its anti-silencing effect at the telomeres, SAS-I also plays a role in repression of the silent mating-type loci *HMR* and *HML* (16,18), and it serves as a boundary factor at *HMR*, where its acetylation of a $tRNA^{Thr}$ gene close to the *HMR*-I silencer helps establish a heterochromatin barrier (19).

Global H4 K16Ac levels in the genome have previously been shown to anti-correlate with transcription over coding regions (20,21). Furthermore, H4 K16Ac, among other histone modifications, was depleted in regions of high histone turnover (22). Since the SAS-I complex performs a large proportion, but not all of total H4 K16Ac [(11,12), data not shown], it was thus of interest to determine which regions (apart from the telomeres) are specifically affected by *sas2Δ*, and where the residual H4 K16Ac that depends on other HATs remains. It is unclear how acetylation by SAS-I is directed to a particular genomic region, for instance to the telomeres. However, SAS-I interacts with the Cac1 subunit of the chromatin assembly factor CAF-I (9). Since CAF-I deposits histones on newly replicated DNA, one can therefore speculate that it recruits SAS-I to sites of chromatin assembly to perform histone acetylation. SAS-I also interacts with the histone chaperone Asf1 (8,9), suggesting that its acetylation activity might be coupled to histone deposition by Asf1.

In this study, we investigated in detail the effect of SAS-I on global H4 K16 acetylation using high-resolution tiling microarrays. Next to its effect at the telomeres, we found a pronounced, genome-wide loss of H4 K16 acetylation specifically in the body of transcribed genes in the absence of Sas2, suggesting a role for SAS-I in transcription elongation. In agreement with this, *sas2Δ* caused resistance to 6-azauracil (6-AU). Furthermore, we observed a higher occupancy of PolII at the 3′-ends of some genes in *sas2Δ*, thus arguing for an increased processivity of PolII in the absence of Sas2. Moreover, Sas2-mediated H4 K16Ac was inversely correlated with the rate of transcription and histone exchange. Altogether, our data suggest a replication-coupled mechanism for H4 K16Ac deposition by SAS-I.

MATERIALS AND METHODS

Strains and media

Yeast strains used in this study are given in Supplementary Table S1. Growth and manipulation of yeast was performed according to standard procedures. Gene knockouts with *kanMX* were performed as described (23). Correct integration was verified in all cases by PCR analysis. Growth assays with 6-AU were performed by supplementing minimal medium with the indicated concentration of 6-AU (stock: 20 mg/ml in 1 M NaOH). Strains used in the 6-AU assay were previously transformed with an *URA3* containing plasmid (pRS316).

Antibodies

The following antibodies were used in this study, α-H4 K16Ac (Upstate Cat. No. #07-329 lot #32214) and α-H4 (Abcam ab31827 lot #386566, #418330) for ChIP-chip; α-H4 K16Ac (Active Motif am39167 #107), α-H4 (Abcam ab31827 lot #418330) and α-PolII (H-224) (Santa Cruz Cat. No. sc-9001) for Chromatin immunoprecipitation (ChIP). All antibodies used in this study were validated for their specificity by western blotting and ChIP analysis in wild-type (wt) and *sas2Δ* strains.

ChIPs and quantitative PCR

All ChIPs were performed at least in triplicate using independent chromatin preparations. ChIPs were carried out essentially as described (24), with the following modifications. Samples were sonicated at 4°C, seven cycles 30 s on and 60 s off. About 4 µl antibody was used per ChIP. RNase (10 mg/ml) digestion was carried out for 1 h at 37°C prior to incubation with proteinase K. DNA clean up was performed with Qiaquick Gel Extraction Kit and ERC cDNA Binding Buffer (Qiagen). Quantitative PCR for the analysis of ChIP samples was performed as described (24) except that SYBR Green Real MasterMix (5 PRIME) was used. Oligonucleotides used for amplification are given in Supplementary Table S2. Significance levels were calculated using student's *t*-test.

For the analysis of PolII association with *pGAL1::FMP27*, cells were grown to mid-exponential phase in galactose-containing medium. They were subsequently shifted to glucose medium, and samples (50 OD cells) were harvested immediately. Cells were cross-linked with 1% formaldehyde for 20 min. ChIP was performed as described above. Relative occupancy of PolII was calculated by dividing the percent of enrichment of the target DNA sequence against PolII enrichment at a steadily transcribed gene, *POL1*. For determining the occupancy of PolII at *PMA1*, cells were grown in full medium with glucose. Cells were harvested (100 OD cells) and crosslinked. ChIP was performed as described above. Oligonucleotide sequences used for amplification are provided in Supplementary Table S2.

Further information on experimental procedures is provided in 'Materials and Methods' section of Supplementary Data.

RESULTS

sas2Δ caused a global reduction of acetylation at H4 K16

Since SAS-I shows activity for H4 K16 *in vitro* (10), we sought to investigate the genome-wide effect of SAS-I loss on H4 K16 acetylation. To this end, ChIPs from wt and *sas2Δ* strains using an antibody against acetylated H4 K16 (H4 K16Ac) were hybridized to high-resolution tiling arrays (ChIP-chip; three biological replicates). In order to normalize for changes in H4 distribution, equivalent ChIP-chip experiments with an antibody against unmodified H4 were performed, and all data in this study show relative H4 K16Ac levels, i.e. H4 K16Ac normalized to H4 levels. A correlation analysis of the relative H4 K16Ac data from *sas2Δ* and wt cells was performed by plotting the relative H4 K16Ac levels in wt against changes in relative H4 K16Ac in *sas2Δ* compared to wt {Figure 1A: H4 K16Ac relative to H4 [*sas2Δ*] minus H4 K16Ac [wt] relative to H4 (*y*-axis) versus H4 K16Ac [wt] relative to H4

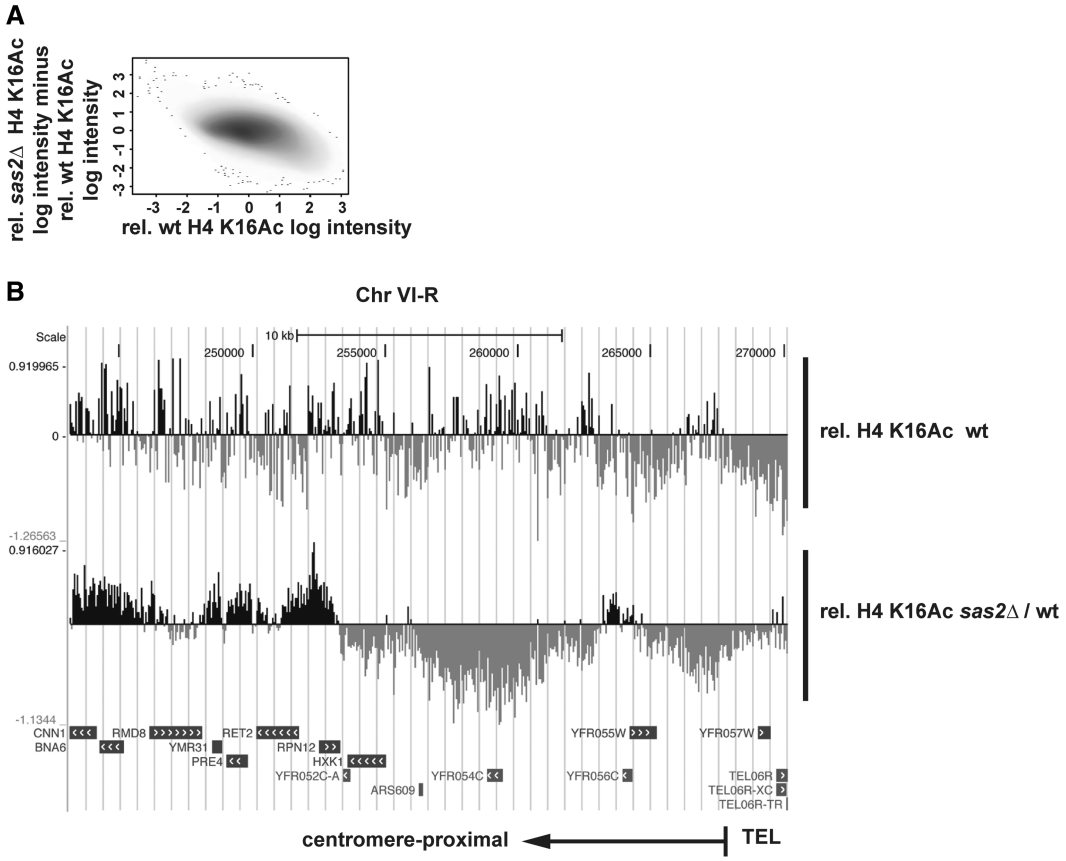

Figure 1. Global H4 K16 acetylation was reduced upon deletion of *SAS2*. (**A**) Correlation analysis of H4 K16Ac relative to H4 (rel. H4 K16Ac) in *sas2Δ* and wt. *X*-axis, H4 K16Ac levels relative to H4 in wt; *y*-axis, relative H4 K16Ac in wt was subtracted from relative H4 K16Ac of *sas2Δ*. (**B**) H4 K16Ac was depleted in subtelomeric regions in *sas2Δ*. H4 K16Ac relative to H4 was averaged over the whole yeast genome for each strain individually. Acetylation signals for wt (top). For *sas2Δ*, the change in relative H4 K16Ac is shown, calculated as relative H4 K16Ac in *sas2Δ* versus relative H4 K16Ac in wt (bottom). Positive signals are indicated as black bars representing above-average H4 K16Ac, negative signals are indicated as grey bars representing below-average acetylation. Twenty-five kilobases of sequence from Chr VI-R is shown. Underlying annotations at the bottom of the graph indicate positions of protein-coding genes and other features according to the *Saccharomyces* Genome Database.

(*x*-axis)}. This analysis showed that *sas2Δ*, as expected, caused a decrease in H4 K16Ac in regions that have high H4 K16Ac in the wt strain, as shown by a trail of the 'cloud' of dots in the graph towards the lower right-hand corner. However, there was also a proportion of the genome that showed no change of H4 K16Ac in *sas2Δ*, as indicated by many dots around the value zero on the *x* and *y* axes. Also, as shown below, the loss of H4 K16Ac was not uniformly distributed over the yeast genome.

The subtelomeric regions are a known target of acetylation by Sas2, where it prevents the spreading of heterochromatin (11,12). Therefore, we investigated these regions for loss of H4 K16Ac in order to validate our ChIP-chip data. For instance, at the right arm of chromosome VI (Figure 1B, top row) and the right arm of chromosome X and III (Supplementary Figure S1A and S1B), we observed a certain level of relative H4 K16Ac in the wt strain (Figure 1B, top row). Acetylation that was higher than average is represented by the black upright bars (positive values), whereas regions with lower than average relative H4 K16Ac are marked by grey, downward bars (negative values). In order to evaluate the effect of *sas2Δ* on H4 K16Ac, we measured the change in relative H4 K16Ac in *sas2Δ* as compared to wt (Figure 1B, second row). The average change over the genome was set to zero (baseline); less-than-average change results in positive values (black bars), and more-than-average change gives negative values (grey bars). In agreement with earlier work (11,12,15), relative H4 K16Ac levels were reduced in *sas2Δ* in subtelomeric regions up to ~20 kB distance from the telomere, for instance at the right arm of chromosome VI (Figure 1B) and the right arm of chromosome X and III (Supplementary Figure S1A and S1B). This conclusion was further supported by a genome-wide analysis (Supplementary Figure S1C), which showed that the change in H4 K16Ac in *sas2Δ* was significantly stronger in subtelomeric than in non-subtelomeric regions. However, as compared to the earlier work, our ChIP-chip data allowed a refined view of local H4 K16Ac levels. Significantly, we did not observe the continuous increase of H4 K16Ac levels in wt towards centromere-proximal sequences reported earlier (11,12)

(Figure 1B, top panel), i.e. there was no 'mound' of H4 K16Ac that has been proposed to inhibit SIR spreading. Also, the decrease of H4 K16Ac in *sas2Δ* was discontinuous (Figure 1B, bottom panel). Thus, our data demonstrated that acetylation by SAS-I was not specifically targeted to subtelomeric regions, for instance by an underlying DNA sequence, and indicated that its distribution in the genome was governed by other, so far unknown principles.

H4 K16Ac was decreased at the 3′-end of long ORFs in *sas2Δ* cells

We next investigated the effect of *sas2Δ* on global H4 K16Ac in non-telomeric regions of the genome. Strikingly, we observed a pronounced depletion of H4 K16Ac specifically within open reading frames (ORFs), but not in intergenic regions in *sas2Δ* cells (Figure 2A, B), a pattern that has gone unnoticed in previous studies because they employed conventional ChIP (11,12), or because they used microarrays based on PCR products (15) rather than the high-resolution tiling arrays used here. We observed that there was less-than-average change in relative H4 K16Ac in *sas2Δ* cells in intergenic regions (black bars in Figure 2A and B) and stronger loss over ORFs (grey bars, Figure 2A and B). This observation was verified using conventional ChIP analysis (Supplementary Figure S1D and data not shown), which showed that the more-than-average changes observed in the ChIP-chip translated to a decrease in H4 K16Ac using conventional ChIP. A quantitation of this observation using box plots (Supplementary Figure S2) showed that the difference in acetylation in *sas2Δ* was strongest over the body of genes and the transcription termination site, rather than in promoter regions.

In order to further evaluate the observed acetylation pattern, the ChIP-chip acetylation data was mapped to relative RNA expression data from wt (Figure 2C) and *sas2Δ* (Figure 2D and E). Transcripts were grouped according to transcript abundance, and genes were normalized to 100% length (for details, see Materials and Methods of Supplementary Data). Unlike acetylation at other sites in H3 or H4, H4 K16Ac in wt did not exhibit a pronounced peak at the 5′ and promoter region of ORFs, but rather showed an increased occupancy along the ORFs, which was consistent with previous studies (21). Furthermore, in wt cells, H4 K16Ac was lower in genes that were transcribed more frequently, whereas genes that were less transcribed showed a higher level of H4 K16Ac (Figure 2C), as has been reported previously (20,21). This analysis suggested that H4 K16Ac was removed from ORFs during transcription.

Our analysis furthermore showed that in *sas2Δ* cells, some H4 K16Ac remained predominantly in the 5′-end of expressed genes (Figure 2D). Of note, the relative H4 K16Ac level in *sas2Δ* cannot be directly compared to the level in wt cells, because the ChIP-chip data was normalized for each strain individually. Because *sas2Δ* causes a decrease, but not complete loss, of bulk H4 K16Ac, the mean acetylation in *sas2Δ* (i.e. the baseline) is likely at a lower level than the mean acetylation in wt. However, investigation of the average change in relative H4 K16Ac in *sas2Δ* as compared to wt (Figure 2E) showed that there was less change in the 5′ region of ORFs, and that the H4 K16Ac depletion was stronger towards the 3′-end of the genes. This effect was more pronounced in genes with lower expression rates than in the most strongly expressed genes (81–100%). A detailed analysis of this observation using box plots showed that this effect was statistically significant (Supplementary Figure S3). In summary, this argued that Sas2-dependent H4 K16Ac was 'fixed' in genes with low transcription rates and thus became most strongly depleted in these genes in the absence of Sas2.

Our visual inspection of the data suggested that the H4 K16Ac pattern in *sas2Δ* cells was more pronounced at long than at short ORFs (Figure 2A, B). To examine this, genes were clustered in two groups according to their H4 K16Ac profile in *sas2Δ* cells (Figure 2F, left and middle). The genes of Group 1 showed a drop of H4 K16Ac predominantly in the second half of the gene, and these genes were significantly longer than the genes of Group 2 (Figure 2F, right panel). The H4 K16Ac profile of Group 2 genes showed an overall higher level of acetylation (Figure 2F, middle panel, *y*-axis) and a less pronounced decrease in the 3′ region as compared to Group 1, and these genes were on average shorter than those of Group 1. Thus, this suggested that the 3′ decrease of H4 K16Ac in *sas2Δ* cells was more pronounced in longer than in shorter genes.

We were concerned that this length effect may be a product of the analysis and techniques applied, rather than being a representation of the *in vivo* H4 K16Ac situation. For instance, it was possible that the ChIP technique was unable to resolve acetylation differences below a certain fragment length. To investigate this, we plotted the relative acetylation levels of the unscaled genes within expression groups that had previously been sorted by length (Supplementary Figures S4–S6). This showed that the remaining relative H4 K16Ac in *sas2Δ* was lower in the 3′ region of long than in short genes of the expression groups. Regardless of the expression group, the remaining acetylation at the 5′-end of long genes was lower than in shorter genes (more blue/green in longer genes versus more yellow/red in shorter genes). This demonstrated that there was not a fixed length of H4 K16Ac remaining in *sas2Δ* cells. In summary, this analysis revealed that H4 K16Ac by SAS-I was most pronounced in the 3′ region of long genes. Thus, the remainder of H4 K16Ac in *sas2Δ* that is deposited by other HATs was present in the 5′ region of the genes, indicating that these HATs operated by different principles than the SAS-I complex.

sas2Δ cells showed resistance to 6-azauracil

Since H4 K16Ac in *sas2Δ* cells was most depleted within ORFs, the region of genes where PolII is in the elongation phase of transcription, we asked whether this was reflected in an effect of *sas2Δ* on transcription elongation by determining the sensitivity of *sas2Δ* cells to 6-azauracil

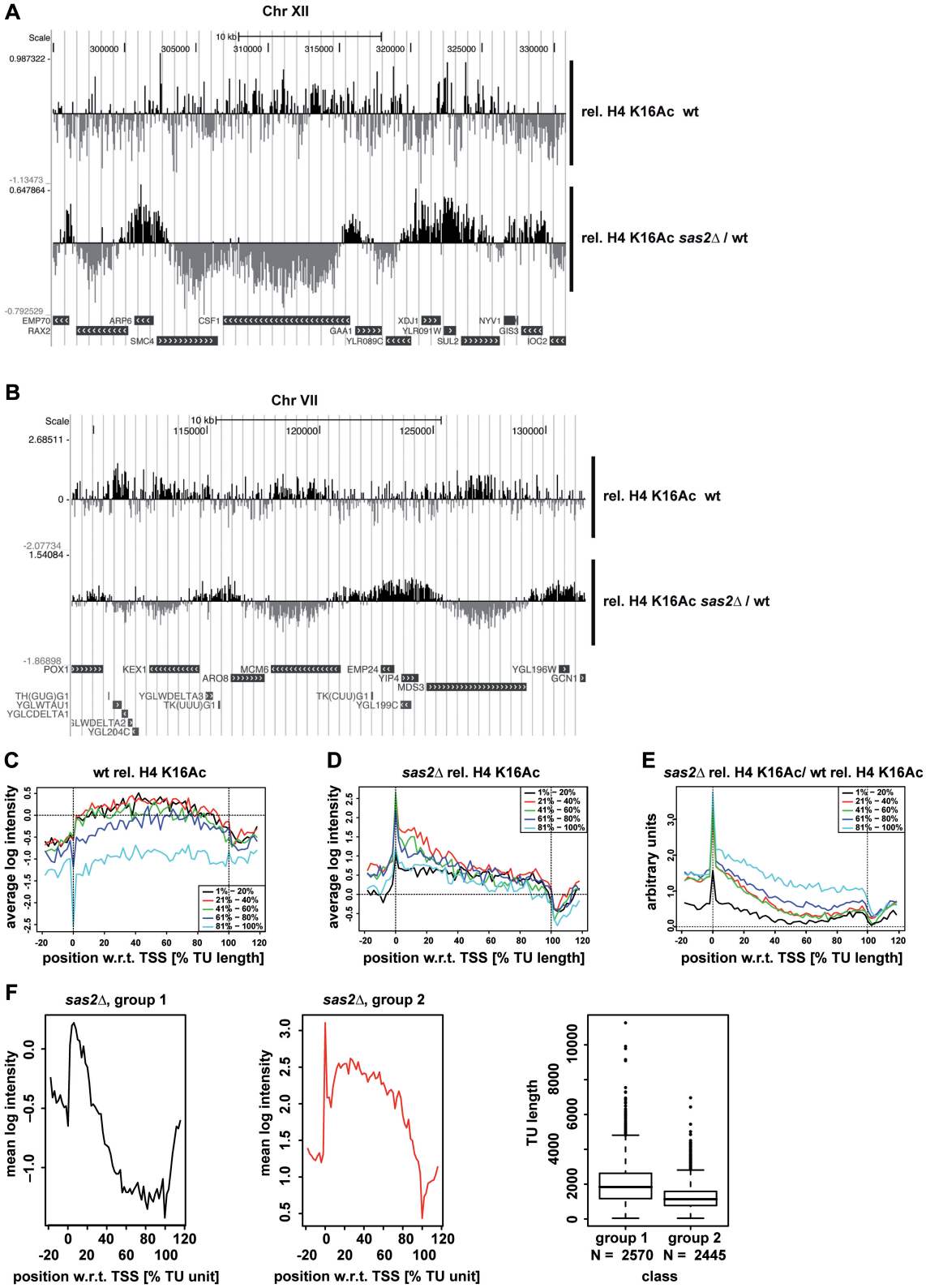

Figure 2. *sas2Δ* caused a genome-wide decrease of H4 K16 acetylation at ORFs. (**A** and **B**) Representative regions of H4 K16Ac depletion at ORFs are presented as in Figure 1B. H4 K16Ac profiling around the *CSF1* gene (A) and a region of Chr VII (B). (**C–E**) Quantitative analysis of H4 K16Ac at ORFs in wt and *sas2Δ*. Yeast genes were binned according to transcription frequency (%) using RNA expression data for wt (C) or *sas2Δ* (D and E), and transcripts were normalized to 100% length. The graph shows the average relative H4 K16Ac of the binned genes in wt (C) and *sas2Δ* (D). Graph E shows the change in relative H4 K16Ac between *sas2Δ* and wt. (**F**) Analysis of the H4 K16Ac profile of *sas2Δ* relative to gene length. Genes were classified by *k*-means clustering. Average relative H4 K16Ac profile of Groups 1 and 2, respectively (left and middle panel). Right, box plot of the average mean length of transcription units of each group. Note that genes belonging to Group 1 were significantly longer than those of Group 2 (P-value < 2.2e-16). Whiskers extend the box 1.5× the box height, dots denote outliers.

(6-AU). 6-AU causes a reduction of the intracellular nucleotide pools and renders PolII unable to elongate efficiently in the absence of transcription elongation factors (25). Conversely, some chromatin remodelling and modification factors, for instance Isw1 (26), or the H3 K36 methyltransferase Set2 (27), cause resistance to 6-AU (Figure 3A and Supplementary Figure S7A). Interestingly, *sas2Δ* cells showed a higher resistance to 6-AU than wt, suggesting that transcription elongation was facilitated in the absence of Sas2 (Figure 3A).

Of note, 6-AU sensitivity can also be obtained by means unrelated to elongation (28), for instance by influencing the expression of drug transporters (29). However, the 6-AU resistance of *sas2Δ* was strongly decreased by deletion of *DST1*, which encodes the elongation factor Dst1 (Figure 3B), demonstrating that it was not due to unspecific effects of Sas2 on drug transport. Since *sas2Δ* also affects telomeric silencing, it was possible that the effect of *sas2Δ* on 6-AU resistance was an indirect effect of increased telomeric silencing. However, the *sas2Δ* 6-AU resistance was independent of *SIR2*, *SIR3* and *SIR4* (Supplementary Figure S7B and S7C), further supporting the notion that the 6-AU resistance was a reflection of an effect on transcription elongation. Furthermore, mutation of H4 K16 to arginine, which mimics the deacetylated state, displayed a 6-AU resistance phenotype similar to that of *sas2Δ* (Supplementary Figure S7D), indicating that Sas2 exerted a repressive effect on transcription elongation through acetylation of H4 K16.

Effect of *sas2Δ* on the processivity of transcription

There are several possibilities for how transcription elongation can be enhanced *in vivo*, namely by affecting the ability of PolII to travel along the entire length of the gene (processivity), the elongation rate *per se*, or the coupling of transcription to subsequent RNA processing events (25). Since the above results suggested a role for Sas2 in transcription elongation, we sought to determine how it affected the distribution and migration of PolII along a gene. For this purpose, we measured the level of PolII association at three positions within the long (8 kB) *FMP27* gene whose expression is driven by the glucose-repressible *GAL1* promoter (25). The kinetics of PolII dissociation was measured after shifting galactose-grown cells to glucose. In wt cells, the level of PolII in galactose along the coding region of *FMP27* was constant (Figure 3C). Unexpectedly, *sas2Δ* cells displayed mildly elevated levels of PolII at the 3′-end of the gene suggestive of an increased accessibility of this region to PolII (Figure 3C). This trend towards an increased level was also observed at two other genes, *PMA1* (Figure 3D) and *YEL025C* (Supplementary Figure S8). However, there was no appreciable difference in the kinetics of PolII dissociation from *FMP27* upon shift of the cells to glucose medium in wt and *sas2Δ* cells (data not shown), indicating that the elongation rate was not affected by Sas2. In conclusion, these experiments suggested that the processivity, but not the elongation rate of PolII increased mildly in the absence of Sas2.

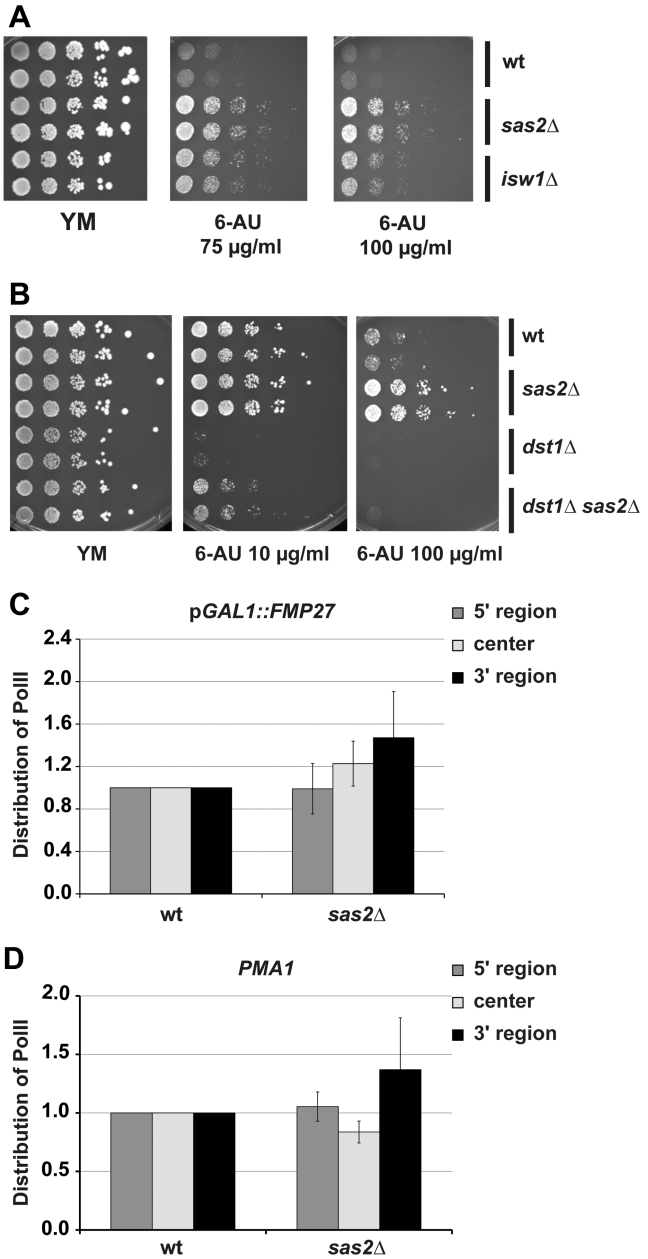

Figure 3. Deletion of *SAS2* caused resistance to 6-azauracil (6-AU). (**A**) *sas2Δ* cells were more 6-AU resistant than *isw1Δ*. Serial dilutions of the indicated strains carrying a *URA3*-marked plasmid where plated on 6-AU containing medium and incubated for 3 days at 30°C. (**B**) *sas2Δ* was epistatic to *dst1Δ*. Representation as in A. (**C** and **D**) PolII was present at higher levels at 3′ region of ORFs in *sas2Δ*. Occupancy of PolII at three indicated positions along *pGAL1::FMP27* (C) and *PMA1* (D) is shown. Cells were grown in galactose (C) or glucose (D), values in wt were normalized to 1.0 at each position and error bars represent standard deviation of three independent replicates.

One prediction from the data above is that in the absence of Sas2, the chromatin might become more loose, which may then lead to increased accessibility to PolII transcription from sequences within the ORF. In line with this notion, we observed genome-wide a mild

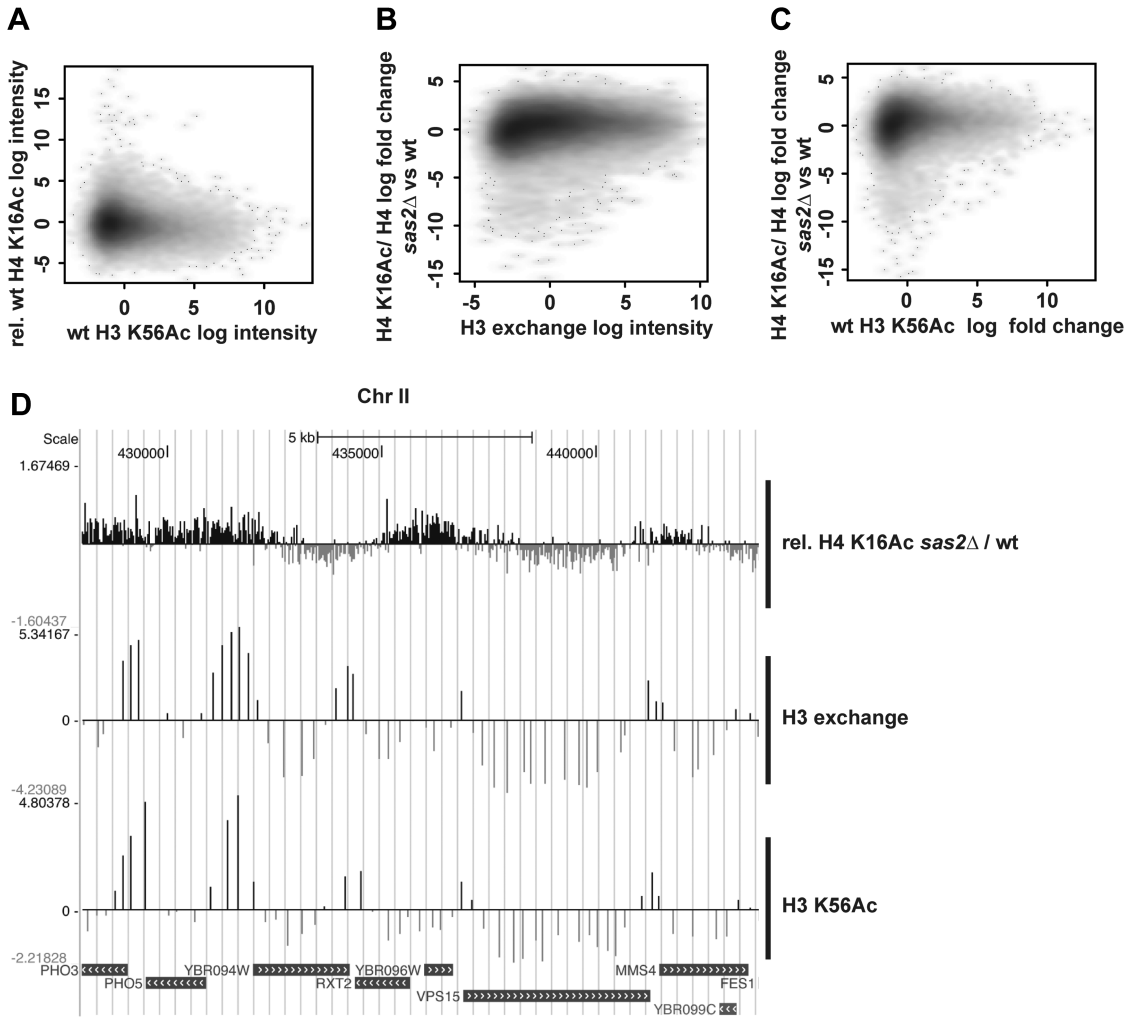

Figure 4. H4 K16Ac was present in regions with low H3 K56 Ac and low histone H3 exchange. (**A–C**) Correlation analysis of wt relative H4 K16Ac and H3 K56Ac (A) and the change in relative H4 K16Ac in *sas2Δ* versus wt and H3 exchange (B) or H3 K56Ac (C) (6). (**D**) Comparison of the change of H4 K16Ac in *sas2Δ* with H3 exchange and H3 K56Ac levels at chromosome II. The data is represented as in Figure 1B.

increase in transcript levels at the 3′-end of genes (Supplementary Figure S9A), and the ratio of 3′ to 5′ transcript levels was moderately increased in *sas2Δ* at selected genes (Supplementary Figure S9B). Furthermore, *sas2Δ* caused increased expression of a *pGAL1*-driven *FLO8-HIS3* reporter construct for cryptic transcription initiation (30), but only when combined with mutations in the elongation factors *SPT6* or *SPT16* (31) (Supplementary Figure S9C and S9D), and *sas2Δ* caused increased resistance to 6-AU in *SPT6* and *SPT16* mutant backgrounds (Supplementary Figure S9E). Thus, *sas2Δ* exerted a mild global effect on the level of transcript from within a gene, and it enhanced the initiation of cryptic transcripts caused by defects in elongation factors.

Since the H3 K36 methyltransferase Set2 has previously been shown to cause cryptic transcription initiation from within genes (27,32), it was of interest to determine whether Set2 exerted this effect via an influence on H4 K16 acetylation. We found a mild reduction of H4 K16Ac in *set2Δ* at the 3′-end of one gene (*CSF1*), but not another (*PMA1*) (Supplementary Figure S10), indicating that there was a partial influence of *set2Δ* on H4 K16Ac at some, but not all genes.

Sas2-dependent H4 K16 acetylation was predominantly found in regions of low histone exchange and low H3 K56 acetylation

Our analysis above showed that Sas2-mediated acetylation was predominantly deposited on long ORFs with a low transcription rate, raising the question as to how this pattern of H4 K16Ac deposition is generated. Of note, low transcription rates are associated with low levels of histone H3 exchange as well as with low levels of H3 K56 acetylation along a gene (6), thus suggesting a correlation between low histone exchange and high levels of Sas2-dependent H4 K16Ac. Importantly, a correlation analysis of our genome-wide H4 K16Ac data from wt cells with H3 K56Ac data (6) revealed that these modifications were mutually exclusive in that regions with high H3 K56Ac showed low H4 K16Ac and vice versa (Figure 4A). Since H3 K56Ac marks sequences with high histone exchange (6), this confirmed the notion that

the histones incorporated during histone exchange were hypoacetylated on H4 K16, as has been reported earlier (22). On the other hand, the observation that low H3 K56Ac, and thus low exchange, correlated with higher H4 K16Ac indicated that K16 acetylation occurred at a time point other than histone exchange. This then raised the question which regions were most affected by loss of Sas2, those with high or those with low histone exchange. A correlation analysis showed that the regions with high H3 exchange (Figure 4B) and high H3 K56Ac (Figure 4C) showed only little change in relative H4 K16Ac, whereas regions with low H3 exchange and H3 K56Ac displayed the most prominent drop in H4 K16Ac in *sas2Δ*. Thus, the same regions within ORFs that displayed low histone exchange and low H3 K56Ac, also showed the strongest loss of H4 K16Ac in *sas2Δ* cells. Conversely, intergenic regions with high H3 exchange were less susceptible to loss of H4 K16Ac in *sas2Δ* (Figure 4D). In conclusion, this showed that Sas2-dependent H4 acetylation was deposited in the genome outside of transcription- and histone exchange-dependent histone turnover.

DISCUSSION

The HAT complex SAS-I has previously been described to acetylate H4 K16 in subtelomeric regions, and that this counteracts the spreading of telomeric heterochromatin (11,12,15). This study substantially refines and expands our view by providing a high-resolution map of global H4 K16Ac by SAS-I. First, our data show that SAS-I acetylation is not specifically targeted to subtelomeric sequences, suggesting that the increase in SIR spreading in *sas2Δ* is the result of increased affinity of the SIR complex to hypoacetylated chromatin rather than to the absence of a specific, local boundary. Secondly, our data reveal the surprising finding that in the absence of Sas2, there is a depletion of H4 K16Ac in the majority of ORFs of the yeast genome, whereas intergenic regions show little dependence on Sas2. Thus, in *sas2Δ* cells, most H4 K16Ac that is deposited by other HATs remains in the promoter and 5′ region of genes. The regions most susceptible to Sas2 acetylation also show low transcription and low histone exchange rates. Thus, a picture emerges where Sas2 acetylation of H4 K16Ac is deposited at a given time/in a given process in the genome, and that this pattern is subsequently 'sculptured' by transcription-independent histone exchange in promoter regions and by passage of the transcription machinery *per se* within ORFs. Thus, SAS-I shows a different mode of operation than other histone-modifying complexes in that it is not recruited to promoters, nor does it migrate along ORFs in association with PolII. Since SAS-I interacts with the chromatin assembly factor CAF-I (9), which performs DNA replication- coupled chromatin assembly, we propose that SAS-I performs genome-wide H4 K16 acetylation during S-phase, in the wake of chromatin assembly. After replication, if transcription and histone exchange rates are low, H4 K16Ac by SAS-I remains in chromatin after deposition. Conversely, if exchange and transcription are high, this will lead to a decrease in H4 K16Ac, because the histones incorporated outside of S-phase and replication-coupled chromatin assembly are under-acetylated on H4 K16. One consequence of this model is that Sas2 might only transiently be associated with chromatin, which is in agreement with the fact that we (data not shown) and others (17,33) have not been able to find Sas2 associated at telomeres of ORFs by ChIP analysis, although this may be due to technical limitations.

Asf1 is an H3/H4 chaperone that mediates transcription-dependent histone exchange (5,6). Interestingly, SAS-I also interacts with Asf1 (8,9), suggesting that SAS-I might perform histone acetylation coupled to Asf1-dependent histone deposition. Future experiments will be required to test this and assess the functional relevance of this interaction.

Since loss of H4 K16Ac in ORFs is so pervasive in *sas2Δ* cells, does this have a global effect on transcription? The most prominent effect of *sas2Δ* is reduced expression of subtelomeric genes due to SIR spreading [(11,12,15), data not shown]. Notably, we also found *sas2Δ* to be resistant to 6-AU, which is indicative of an effect on transcription elongation (25). However, this did not translate easily to a biochemically measurable variable. We found a mild increase in PolII processivity, but no change in PolII elongation rate, and the level of transcript from the 3′-end of genes was slightly higher in *sas2Δ*. However, this effect seemed to be distinct from the initiation of cryptic transcripts from within genes, which leads to the generation of shorter transcripts at selected genes that have a defined start site and a defined length (30,31). Also, the increase of 3′ transcript levels in *sas2Δ* was milder than that observed in other cryptic initiation mutants like *set2Δ*, or in the absence of the HDAC complex Rpd3(S) (32), and unlike *set2Δ* or the deletion of Rpd3 complex components, *sas2Δ* exacerbated the cryptic initiation defect of mutations in *SPT6* and *SPT16* at a *FLO8::HIS3* reporter construct, but had no effect on its own. In sum, these results suggested distinct mechanisms of altering transcription between SAS-I and other factors affecting cryptic initiation, and the exact nature of this alteration by SAS-I is unclear.

We furthermore observed a more pronounced loss of H4 K16Ac at long than at short genes in *sas2Δ*. One possibility is that acetylation in the 5′ region of short genes is performed by different HAT(s) than that of long genes, and that this/these HATs have a broader range of acetylation. Alternatively, there may be differences in transcription-coupled acetylation on long versus short genes that become evident in the absence of Sas2. Which HATs contribute to the remainder of H4 K16Ac in *sas2Δ* is unclear. There is a partial contribution of Esa1/NuA4 to H4 K16Ac at telomeres (12), but bulk H4 K16Ac is not decreased in *esa1* mutants (11,34). Thus, a systematic analysis of H4 K16Ac in *sas2Δ* mutants combined with deletions in other HATs will be required to identify the enzymes responsible for residual H4 K16Ac in *sas2Δ*.

What purpose does genome-wide Sas2-dependent H4 K16 acetylation serve? Perhaps this is a way to mark the chromatin as duplicated after DNA replication and chromatin assembly, thus maintaining it in a

euchromatic state. Since H4 K16Ac prevents SIR binding (13), instituting this mark in S-phase might prevent inappropriate SIR binding in other regions of the genome particularly during the process of chromatin assembly, when histone modifications otherwise are diluted.

In summary, this study reveals a novel global role for SAS-I-mediated histone acetylation in ORFs throughout the genome and relates it to histone exchange and transcription elongation. H4 K16Ac has previously been linked to elongation in other organisms. However, in mammalian cells, phosphorylation of H3 Ser10 during transcriptional activation leads to the recruitment of MOF, which is a close homologue of Sas2 and a HAT for H4 K16. This in turn modulates transcription elongation via recruitment of BRD4 (35). Furthermore, MOF in *Drosophila* directly binds in a bimodal fashion to the promoters and 3′-end of dosage-compensated genes on the male X-chromosome and increases their expression (36). Thus, MOF in these organisms is targeted to its site of action using a different mechanism than SAS-I in yeast. Therefore, although these enzymes are structurally homologous and show the same substrate specificity, there are important species-specific mechanistic differences in their function and effect on chromatin.

SUPPLEMENTARY DATA

Supplementary Data are available at NAR Online.

ACKNOWLEDGEMENTS

We wish to thank F. Winston and A. Nourani for strains, S. Clauder-Münster for the hybridization of the RNA expression arrays and K. Nicklasch, C. Vole, M. Rübeling and R. Hohmeister for excellent technical assistance. We further thank the Ehrenhofer-Murray lab for many stimulating discussions.

FUNDING

Deutsche Forschungsgemeinschaft (DFG; EH 237/5-1); Universität Duisburg-Essen (UDE). Funding for open access charge: DFG, UDE.

Conflict of interest statement. None declared.

REFERENCES

1. Kurdistani,S.K. and Grunstein,M. (2003) Histone acetylation and deacetylation in yeast. *Nat. Rev. Mol. Cell. Biol.*, **4**, 276–284.
2. Roth,S.Y., Denu,J.M. and Allis,C.D. (2001) Histone acetyltransferases. *Annu. Rev. Biochem.*, **70**, 81–120.
3. Shilatifard,A., Conaway,R.C. and Conaway,J.W. (2003) The RNA polymerase II elongation complex. *Annu. Rev. Biochem.*, **72**, 693–715.
4. Belotserkovskaya,R., Oh,S., Bondarenko,V.A., Orphanides,G., Studitsky,V.M. and Reinberg,D. (2003) FACT facilitates transcription-dependent nucleosome alteration. *Science*, **301**, 1090–1093.
5. Schwabish,M.A. and Struhl,K. (2006) Asf1 mediates histone eviction and deposition during elongation by RNA polymerase II. *Mol. Cell*, **22**, 415–422.
6. Rufiange,A., Jacques,P.E., Bhat,W., Robert,F. and Nourani,A. (2007) Genome-wide replication-independent histone H3 exchange occurs predominantly at promoters and implicates H3 K56 acetylation and Asf1. *Mol. Cell*, **27**, 393–405.
7. Kim,J.A. and Haber,J.E. (2009) Chromatin assembly factors Asf1 and CAF-1 have overlapping roles in deactivating the DNA damage checkpoint when DNA repair is complete. *Proc. Natl Acad. Sci. USA*, **106**, 1151–1156.
8. Osada,S., Sutton,A., Muster,N., Brown,C.E., Yates,J.R. 3rd, Sternglanz,R. and Workman,J.L. (2001) The yeast SAS (something about silencing) protein complex contains a MYST-type putative acetyltransferase and functions with chromatin assembly factor ASF1. *Genes Dev.*, **15**, 3155–3168.
9. Meijsing,S.H. and Ehrenhofer-Murray,A.E. (2001) The silencing complex SAS-I links histone acetylation to the assembly of repressed chromatin by CAF-I and Asf1 in Saccharomyces cerevisiae. *Genes Dev.*, **15**, 3169–3182.
10. Sutton,A., Shia,W.J., Band,D., Kaufman,P.D., Osada,S., Workman,J.L. and Sternglanz,R. (2003) Sas4 and Sas5 are required for the histone acetyltransferase activity of Sas2 in the SAS complex. *J. Biol. Chem.*, **278**, 16887–16892.
11. Kimura,A., Umehara,T. and Horikoshi,M. (2002) Chromosomal gradient of histone acetylation established by Sas2p and Sir2p functions as a shield against gene silencing. *Nat. Genet.*, **32**, 370–377.
12. Suka,N., Luo,K. and Grunstein,M. (2002) Sir2p and Sas2p opposingly regulate acetylation of yeast histone H4 lysine16 and spreading of heterochromatin. *Nat. Genet.*, **32**, 378–383.
13. Rusche,L.N., Kirchmaier,A.L. and Rine,J. (2003) The establishment, inheritance, and function of silenced chromatin in Saccharomyces cerevisiae. *Annu. Rev. Biochem.*, **72**, 481–516.
14. Ehrentraut,S., Weber,J.M., Dybowski,J.N., Hoffmann,D. and Ehrenhofer-Murray,A.E. (2010) Rpd3-dependent boundary formation at telomeres by removal of Sir2 substrate. *Proc. Natl Acad. Sci. USA*, **107**, 5522–5527.
15. Shia,W.J., Li,B. and Workman,J.L. (2006) SAS-mediated acetylation of histone H4 Lys 16 is required for H2A.Z incorporation at subtelomeric regions in Saccharomyces cerevisiae. *Genes Dev.*, **20**, 2507–2512.
16. Reifsnyder,C., Lowell,J., Clarke,A. and Pillus,L. (1996) Yeast SAS silencing genes and human genes associated with AML and HIV-1 Tat interactions are homologous with acetyltransferases. *Nat. Genet.*, **14**, 42–49.
17. Dang,W., Steffen,K.K., Perry,R., Dorsey,J.A., Johnson,F.B., Shilatifard,A., Kaeberlein,M., Kennedy,B.K. and Berger,S.L. (2009) Histone H4 lysine 16 acetylation regulates cellular lifespan. *Nature*, **459**, 802–807.
18. Ehrenhofer-Murray,A.E., Rivier,D.H. and Rine,J. (1997) The role of Sas2, an acetyltransferase homologue of Saccharomyces cerevisiae, in silencing and ORC function. *Genetics*, **145**, 923–934.
19. Donze,D. and Kamakaka,R.T. (2001) RNA polymerase III and RNA polymerase II promoter complexes are heterochromatin barriers in Saccharomyces cerevisiae. *EMBO J.*, **20**, 520–531.
20. Kurdistani,S.K., Tavazoie,S. and Grunstein,M. (2004) Mapping global histone acetylation patterns to gene expression. *Cell*, **117**, 721–733.
21. Liu,C.L., Kaplan,T., Kim,M., Buratowski,S., Schreiber,S.L., Friedman,N. and Rando,O.J. (2005) Single-nucleosome mapping of histone modifications in S. cerevisiae. *PLoS Biol.*, **3**, e328.
22. Dion,M.F., Kaplan,T., Kim,M., Buratowski,S., Friedman,N. and Rando,O.J. (2007) Dynamics of replication-independent histone turnover in budding yeast. *Science*, **315**, 1405–1408.
23. Wach,A. (1996) PCR-synthesis of marker cassettes with long flanking homology regions for gene disruptions in S. cerevisiae. *Yeast*, **12**, 259–265.
24. Weber,J.M., Irlbacher,H. and Ehrenhofer-Murray,A.E. (2008) Control of replication initiation by the Sum1/Rfm1/Hst1 histone deacetylase. *BMC Mol. Biol.*, **9**, 100.
25. Mason,P.B. and Struhl,K. (2005) Distinction and relationship between elongation rate and processivity of RNA polymerase II in vivo. *Mol. Cell*, **17**, 831–840.

26. Morillon,A., Karabetsou,N., O'Sullivan,J., Kent,N., Proudfoot,N. and Mellor,J. (2003) Isw1 chromatin remodeling ATPase coordinates transcription elongation and termination by RNA polymerase II. *Cell*, **115**, 425–435.
27. Keogh,M.C., Kurdistani,S.K., Morris,S.A., Ahn,S.H., Podolny,V., Collins,S.R., Schuldiner,M., Chin,K., Punna,T., Thompson,N.J. *et al*. (2005) Cotranscriptional set2 methylation of histone H3 lysine 36 recruits a repressive Rpd3 complex. *Cell*, **123**, 593–605.
28. Riles,L., Shaw,R.J., Johnston,M. and Reines,D. (2004) Large-scale screening of yeast mutants for sensitivity to the IMP dehydrogenase inhibitor 6-azauracil. *Yeast*, **21**, 241–248.
29. Garcia-Lopez,M.C., Miron-Garcia,M.C., Garrido-Godino,A.I., Mingorance,C. and Navarro,F. (2010) Overexpression of SNG1 causes 6-azauracil resistance in Saccharomyces cerevisiae. *Curr. Genet*., **56**, 251–263.
30. Cheung,V., Chua,G., Batada,N.N., Landry,C.R., Michnick,S.W., Hughes,T.R. and Winston,F. (2008) Chromatin- and transcription-related factors repress transcription from within coding regions throughout the Saccharomyces cerevisiae genome. *PLoS Biol*, **6**, e277.
31. Kaplan,C.D., Laprade,L. and Winston,F. (2003) Transcription elongation factors repress transcription initiation from cryptic sites. *Science*, **301**, 1096–1099.
32. Carrozza,M.J., Li,B., Florens,L., Suganuma,T., Swanson,S.K., Lee,K.K., Shia,W.J., Anderson,S., Yates,J., Washburn,M.P. *et al*. (2005) Histone H3 methylation by Set2 directs deacetylation of coding regions by Rpd3S to suppress spurious intragenic transcription. *Cell*, **123**, 581–592.
33. Jacobson,S. and Pillus,L. (2009) The SAGA subunit Ada2 functions in transcriptional silencing. *Mol. Cell. Biol*., **29**, 6033–6045.
34. Suka,N., Suka,Y., Carmen,A.A., Wu,J. and Grunstein,M. (2001) Highly specific antibodies determine histone acetylation site usage in yeast heterochromatin and euchromatin. *Mol. Cell*, **8**, 473–479.
35. Zippo,A., Serafini,R., Rocchigiani,M., Pennacchini,S., Krepelova,A. and Oliviero,S. (2009) Histone crosstalk between H3S10ph and H4K16ac generates a histone code that mediates transcription elongation. *Cell*, **138**, 1122–1136.
36. Kind,J., Vaquerizas,J.M., Gebhardt,P., Gentzel,M., Luscombe,N.M., Bertone,P. and Akhtar,A. (2008) Genome-wide analysis reveals MOF as a key regulator of dosage compensation and gene expression in Drosophila. *Cell*, **133**, 813–828.